Abrupt change of Antarctic moisture origin at the end of Termination II

Valérie Masson-Delmotte, Barbara Stenni, Thomas Blunier, Olivier Cattani, Jérôme Chappellaz, H. Cheng, G. Dreyfus, R.L. Edwards, Sonia Falourd, Aline Govin, et al.

Abrupt change of Antarctic moisture origin at the end of Termination II

V. Masson-Delmotte[a,1], B. Stenni[b], T. Blunier[c], O. Cattani[a], J. Chappellaz[d], H. Cheng[e], G. Dreyfus[a], R. L. Edwards[e], S. Falourd[a], A. Govin[a], K. Kawamura[f], S. J. Johnsen[c], J. Jouzel[a], A. Landais[a], B. Lemieux-Dudon[d], A. Lourantou[d], G. Marshall[g], B. Minster[a], M. Mudelsee[h,i], K. Pol[a], R. Röthlisberger[g,2], E. Selmo[j], and C. Waelbroeck[a]

[a]Laboratoire des Sciences du Climat et de l'Environnement (Institut Pierre Simon Laplace/Commissariat à l'Energie Atomique—Centre National de la Recherche Scientifique—Université Versailles St-Quentin Unité Mixte de Recherche 8212), L'Orme des Merisiers, CEA Saclay, 91191 Gif-sur-Yvette cédex, France; [b]Department of Geosciences, University of Trieste, I-34127 Trieste, Italy; [c]Centre for Ice and Climate, Niels Bohr Institute, University of Copenhagen, Juliane Maries Vej 30, DK 2100, Copenhagen, Denmark; [d]Laboratoire de Glaciologie et de Géophysique de l'Environnement (Centre National de la Recherche Scientifique—Université Joseph Fourier 5183), 54 rue Molière, 38402 Saint Martin d'Hères cédex, France; [e]Department of Geology and Geophysics, University of Minnesota, 310 Pillsbury Drive Southeast, Minneapolis, MN 55455-1333; [f]National Institute of Polar Research, Research Organization of Information and Systems, 10-3 Midorichou, Tachikawa, Tokyo 190-8518, Japan; [g]British Antarctic Survey, Natural Environment Research Council, Cambridge, CB3 0ET, United Kingdom; [h]Alfred Wegener Institute for Polar and Marine Research, Climate Science Division, Bussestrasse 24, 25570 Bremerhaven, Germany; [i]Climate Risk Analysis, Schneiderberg 26, 30167 Hannover, Germany; and [j]Department of Earth Sciences, University of Parma, I-43100 Parma, Italy

Edited by David Hodell, University of Florida, Department of Geosciences, Gainesville, FL, and accepted by the Editorial Board June 1, 2010 (received for review December 18, 2009)

The deuterium excess of polar ice cores documents past changes in evaporation conditions and moisture origin. New data obtained from the European Project for Ice Coring in Antarctica Dome C East Antarctic ice core provide new insights on the sequence of events involved in Termination II, the transition between the penultimate glacial and interglacial periods. This termination is marked by a north–south seesaw behavior, with first a slow methane concentration rise associated with a strong Antarctic temperature warming and a slow deuterium excess rise. This first step is followed by an abrupt north Atlantic warming, an abrupt resumption of the East Asian summer monsoon, a sharp methane rise, and a CO_2 overshoot, which coincide within dating uncertainties with the end of Antarctic optimum. Here, we show that this second phase is marked by a very sharp Dome C centennial deuterium excess rise, revealing abrupt reorganization of atmospheric circulation in the southern Indian Ocean sector.

last interglacial | paleoclimate | westerlies

The previous interglacial period appears unusually warm in Antarctica, as recorded in the water stable isotopes (δD or δ^{18}O) from Vostok (1), Dome Fuji (2), and European Project for Ice Coring in Antarctica (EPICA) Dome C (EDC) (3) ice cores. In the context of the past 800 kyr, Termination II—the transition from the penultimate glacial to the previous interglacial—is associated with the largest glacial–interglacial Antarctic temperature increase. The maximum EDC δD is reached ~129 ka (thousand years before present), at the end of Termination II and the onset of Marine Isotopic Stage (MIS) 5e (3). Such early interglacial optima are a characteristic of the past five interglacial periods in Antarctica. Sensitivity studies conducted with coupled ocean-atmosphere climate models reveal that this warming cannot be explained by the climate response to MIS5e orbital forcing only (4). Changes in ocean circulation linked with the final northern hemisphere deglaciation have been suggested to cause the early Antarctic warming (4). With a focus on the last two terminations, we thus explore the links between Antarctic early interglacial warmth and the preceding deglacial history and show that Termination II is marked by an abrupt change in the oceanic evaporative sources providing moisture at the EDC Antarctic site.

Termination I is marked by an early resumption of the Atlantic Meridional Overturning Circulation (AMOC) (5) after the Heinrich 1 event (massive north Atlantic ice rafted debris event, Fig. 1*I*) leading to the Bølling-Allerød (B-A) warming in the northern hemisphere (Fig. 1 *F* and *G*). This abrupt warming is followed by an abrupt return to cold, quasi-glacial conditions. The Younger Dryas (YD) cold interval is likely caused by a freshening of the northern North Atlantic and a collapse of the AMOC (5, 6). Termination I abrupt events are also strongly imprinted in East Asian summer monsoon (EASM) activity (Fig. 1*D*) (7) and atmospheric methane concentrations (Fig. 1*E*) (8). During Termination I, the EDC δD (Fig. 1*B*) undergoes a first increase toward the Antarctic Isotopic Maximum AIM1, interrupted by the Antarctic Cold Reversal—the counter part of B-A warming, and followed by a second increase toward an early Holocene optimum peak (AIM0), which coincides with the AMOC resumption at the end of YD (5).

By contrast, EDC δD (Fig. 2*B*) shows a steady increase along Termination II. This termination is marked by the occurrence of the Heinrich 11 (H11) event (Fig. 2*H*) ending when the Antarctic temperature has already reached interglacial levels, and a likely reduced AMOC for the duration of the deglaciation (9, 10). Although there is evidence for reversals in some records of sea level (11), in eastern North Atlantic ocean surface temperature (12), and a short interstadial (Chinese interstadial B.1, lasting several centuries at ~134 ka, thousand years before present) in the EASM (7), most northern hemisphere records display cold conditions during H11 (phase 1) followed by a sharp temperature rise at ~129 ka (9) (phase 2). Within dating uncertainties (*SI Appendix B*), the rapid northern hemisphere temperature rise coincides with an abrupt increase in atmospheric methane (Fig. 2*E*) (8), suggested to be linked with an abrupt resumption of the EASM (Fig. 2*D*) (13). As during Termination I, the abrupt northern hemisphere warming (Fig. 2 *F* and *G*) coincides with the end of the Antarctic temperature optimum, in a bipolar seesaw pattern. Between their peak warmth and the following cooling, AIM0 and 1 and this Termination II AIM are indeed fully comparable in magnitude (typically 1–2 °C) and in duration to

Author contributions: V.M.-D., J.C., R.L.E., A.G., A. Landais, and B.L.-D. designed research; V.M.-D., B.S., T.B., O.C., J.C., H.C., G.D., R.L.E., A.G., K.K., S.J.J., J.J., A. Landais, B.L.-D., A. Lourantou, M.M., K.P., R.R., E.S., and C.W. performed research; V.M.-D., B.S., T.B., O.C., J.C., H.C., G.D., R.L.E., S.F., A.G., S.J.J., J.J., A. Landais, A. Lourantou, G.M., B.M., M.M., K.P., R.R., E.S., and C.W. analyzed data; and V.M.-D., B.S., T.B., J.C., H.C., R.L.E., A.G., K.K., J.J., A. Landais, G.M., M.M., R.R., and C.W. wrote the paper.

The authors declare no conflict of interest.

This article is a PNAS Direct Submission. D.H. is a guest editor invited by the Editorial Board.

[1]To whom correspondence should be addressed. E-mail: valerie.masson@cea.fr.

[2]Present address: Federal Office for the Environment, Climate Division, CH-3003 Bern, Switzerland.

This article contains supporting information online at www.pnas.org/lookup/suppl/doi:10.1073/pnas.0914536107/-/DCSupplemental.

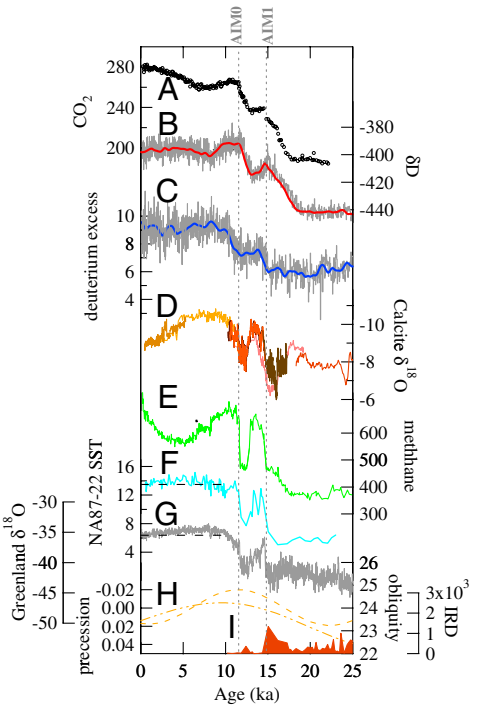

Fig. 1. Comparison of records of Termination I. A coherent Greenland and Antarctic glaciological age scale is used (36). From top to bottom, (*A*) CO_2 concentration [ppm by volume, from Vostok, crosses (1), and from EDC (28, 37) circles]; (*B*) EDC δD (3) (‰, light gray); and *C*) deuterium excess (‰ against Vienna Standard Mean Ocean Water). Raw data measured along 55-cm samples were measured with a mean analytical precision of 0.5‰ at Laboratoire des Sciences du Climat et de l'Environnement (δD, dark gray), 0.05‰ at Trieste and Parma (δ^{18}O) giving access to deuterium excess (*Bottom*, gray). Smoothed records (δD, thick red; excess, thick blue) were produced from a nine-point binomial filter using 100-yr resampled data. Dashed vertical lines highlight abrupt deuterium excess rises during Termination I (AXR1a and AXR1b) detected using the RAMPFIT change-point regression method (see *SI Appendix B*). (*D*) Chinese Asian monsoon speleothem calcite δ^{18}O [Hulu and Sanbao caves (7); different speleothem records available for Termination I are displayed with different colors of orange)]. (*E*) EPICA Dome C methane data (ppb by volume) from EPICA Dome C (thick green) (8). (*F*) North Atlantic SST (blue, Celsius) from cores NA87-22 (38) (see *SI Text*). (*G*) Greenland NorthGRIP ice core δ^{18}O, a proxy of Greenland temperature (see *SI Appendix B*). (*H*) Variations of obliquity (dotted dashed yellow line) and precession parameter (dashed yellow line) (reversed axis to be in phase with Northern Hemisphere summer insolation) are also displayed. (*I*) Ice rafted detritus (IRD) (lithics/g dry sediment) (brown) data from core NA87-22 (38, 39). Long-dashed horizontal lines display the late Holocene temperature levels.

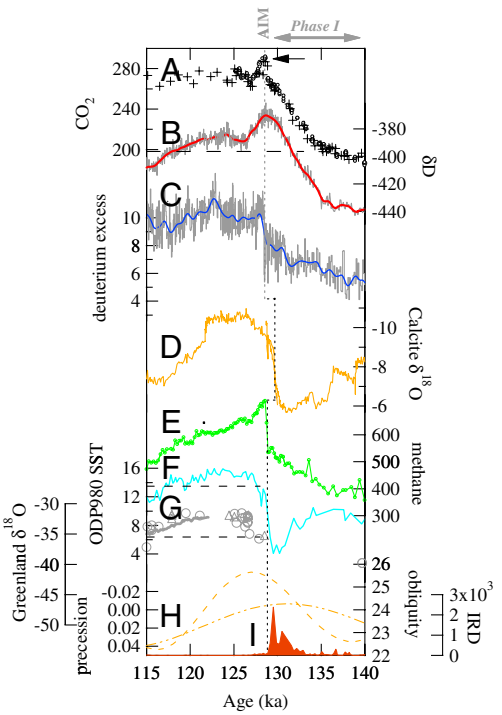

Fig. 2. Same as Fig. 1 but for Termination II. The EDC3 age scale (40) is used as a reference for Termination II for marine and ice core records. The two phases of Termination II are highlighted above the upper horizontal axis (phase 1 and AIM), as well as the CO_2 overshoot (black arrow). Dashed vertical lines highlight the abrupt deuterium excess rise during Termination II (AXR2) detected using the RAMPFIT change-point regression method (see *SI Appendix B*). In *F*, SST data from marine core ODP 980 (9) are displayed. In *G*, Greenland ice core δ^{18}O, a proxy of Greenland temperature, is reconstructed from Greenland Ice Core Project (GRIP), Greenland Ice Sheet Project 2 (GISP2), and NorthGRIP ice cores (see *SI Appendix B*). In *I*, IRD data are obtained from core ODP 980 (9). Long-dashed horizontal lines display the late Holocene temperature levels for comparison with MIS5.5 temperatures.

the glacial AIM events, attributed to the bipolar seesaw linked with changes in the AMOC (14).

Combined δD and δ^{18}O measurements conducted on the same samples of the EDC ice core have provided deuterium excess data ($d = \delta D - 8\delta^{18}O$) and new insights on Dome C moisture source over the Holocene, the last deglaciation, and the last glacial period (15). Deuterium excess (16, 17) is an integrated tracer of the water cycle mainly influenced by kinetic fractionation effects taking place at the moisture source during evaporation, but also during droplet reevaporation and formation of ice crystals (*SI Appendix A*). The EDC deuterium excess record is now extended back to Termination II (Figs. 2*C* and 3) at much higher resolution (~50 yr) than the earlier Antarctic ice core data from Vostok (16) and Dome Fuji (18). Modeling studies using back trajectories as well as atmospheric general circulation models suggest that Dome C receives moisture transported from the temperate area of the southern Indian Ocean in contrast to other East Antarctic sites such as Vostok or Dome F, expected to receive a larger contribution from the Atlantic or Pacific subtropics (19). Simulations show that the interglacial deuterium excess in central Antarctica is strongly linked with changes in the Southern Annular Mode (SAM) (20), as reduced westerlies weaken high-latitude evaporation and permit stronger advection of midlatitude moisture toward central Antarctica, resulting in a warmer moisture source and higher deuterium excess in modeled central Antarctica precipitation. Changes in EDC deuterium excess data therefore reflect both changes in evaporation conditions in its moisture source region and geographical shifts in moisture origin in relationship with atmospheric circulation. Our record adds to the understanding of climate dynamics by documenting changes affecting the south Indian Ocean area, with an unprecedented resolution over MIS5.5–6.

Termination II starts after ~140 ka, when Antarctic temperature (δD), deuterium excess, methane, and carbon dioxide start increasing from low glacial values (Fig. 2). The first warming phase (δD increase) is paralleled by a slow deuterium excess rise. The Antarctic warming is mimicked by parallel Austral ocean warming at mid and high latitudes (21–23). This small deuterium excess rise is interpreted as resulting from the compensation between a warming southern Indian Ocean (inducing higher excess) and an increasing contribution of high latitudes to EDC moisture (inducing a lower excess). In a second phase, when δD reaches an optimum, deuterium excess undergoes a drastic shift, at ~128.5 ka. This abrupt excess rise (AXR) event reaches a magnitude of 2.4‰ (half of glacial–interglacial amplitudes) within approximately a century (*SI Appendix B*), much larger than other secondary (~1‰) deuterium excess variations (detected

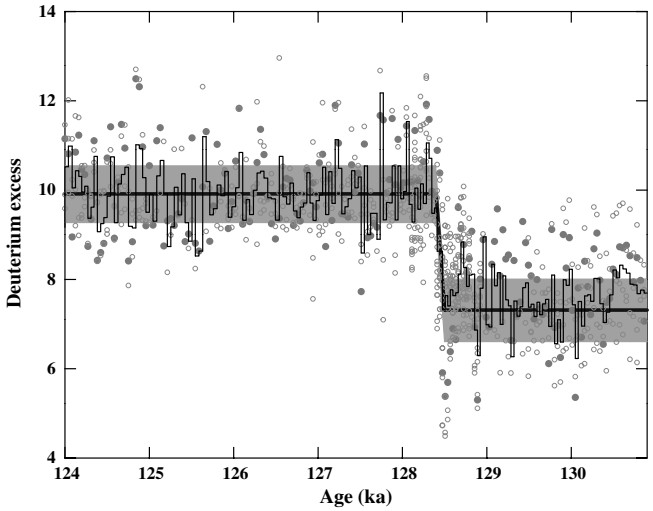

Fig. 3. Rapid deuterium excess shift during Termination II (‰) as a function of EDC3 age (ka). Repeated measurements of δD and δ^{18}O have been conducted in different laboratories (Saclay and Parma for δD, Trieste and Copenhagen for δ^{18}O) on each 55-cm length interval using "bag" samples (55 cm) and the average of five successive "fine cut" samples (11 cm), giving between 2 and 16 independent estimates of deuterium excess values. The deuterium excess calculated from the initial bag sample δD values (3) is displayed as filled circles (Figs. 1 and 2), and the other data as open circles. The average value obtained for each 55-cm depth is displayed as a black stair step. The ramp transition as well as the mean levels before and after this transition are displayed as thick lines. The average quadratic analytical uncertainty ($\pm$0.8‰) is shown as the shading. On this specific set of data, the standard deviation amongst the absolute values of the differences between replicate measurements is 0.8‰ for δD, 0.1‰ for δ^{18}O, and 0.8‰ for deuterium excess.

around 130 and 122.5 ka). The AXR event was not identified in the ~10 times lower resolution Vostok record (16). Within a few centuries, it appears to coincide with the abrupt changes in methane concentration (8) (*SI Appendix B*) and in EASM circulation detected in Chinese speleothems (7, 13) (now dated at 129.0 $\pm$ 0.1 ka) (13). The approximate centennial duration of the EASM shift (13) is also similar to the duration of the AXR. The AXR event is robust with respect to corrections for sea water isotopic composition and site and source temperature inversion (15, 17). This AXR event is both faster and larger than the two multicentennial deuterium excess increases occurring during Termination I, associated respectively with the beginning of the Antarctic Cold Reversal and the end of the Early Holocene optimum (17) (see *SI Appendix B*).

Discussion

The abrupt AXR event cannot be explained by the progressive increase in south Indian ocean sea surface temperature (SST) documented in marine records (21–23), and must therefore reflect an abrupt geographical shift of the moisture origin toward warmer evaporation conditions linked with changes in atmospheric water vapor transport in the south Indian Ocean sector. This AXR event is evidence for a centennial shift in atmospheric moisture transport to Antarctica. Marine cores (24, 25), climate models, and ice core aerosol data (26) point to a weakening of westerlies across Terminations. The sharp deuterium excess increase reflects a rapid shift of Dome C moisture source to lower latitudes likely enabled by abruptly reduced westerlies (20, 27), which may also be involved in the parallel overshoot in atmospheric CO_2 concentration (28).

The present-day interannual climate variability has revealed an interhemispheric link between high southern latitude atmospheric circulation and EASM. Today, strong westerlies characterized by a positive September–November SAM index induce warm September–February subtropical South Indian Ocean SSTs, followed by warm May–July SSTs in the equatorial Indian Ocean and Bay of Bengal. This sequence results in a weak EASM (29). During the last interglacial, the abrupt shifts in north Atlantic SSTs (9), EASM, atmospheric methane concentration, and EDC deuterium excess occur simultaneously (within age scale uncertainties, see *SI Appendix B*), which cannot be coincidence. The simultaneous shifts recorded in AXR and EASM points to an interhemispheric coupling between the south Indian Ocean atmospheric dynamics and EASM during MIS5.5.

Modeling studies show that AMOC reacts strongly to North Atlantic meltwater flux with widespread impacts on atmospheric circulation both in EASM and in the southern hemisphere (30). During Termination I, slow changes in EDC moisture indeed occur during intervals of AMOC resumption. However, Terminations I and II have different orbital, deglacial, and AMOC histories. The melting of northern ice sheets persistent along Termination II into the early last interglacial delays the full establishment of a vigorous AMOC. Paleoceanographic data show that the complete AMOC recovery of an interglacial AMOC below ~3000 m occurred at ~124 ka in the EDC3 timescale (10, 31). However, benthic δ^{13}C data from shallower North Atlantic cores indicate that AMOC resumption above that depth occurred between 130 and 128 ka (31), i.e., simultaneously, within age uncertainties, with the AXR event and the sharp increase in EASM. The later establishment of a vigorous interglacial AMOC at depth results from the northern high-latitude climatic response to high boreal summer insolation (10, 31).

Conclusions

Our synchronization clearly shows that the strong Antarctic optimum at ~130 ka is occurring during northern hemisphere deglaciation and shows similarities with glacial bipolar seesaw events. The deuterium excess data strongly suggest that changes in the southern hemisphere atmospheric circulation are at play at the end of this Antarctic warm interval. Were these southern changes purely driven by the final resumption of AMOC? Or was there a role for interhemispheric atmospheric transport from the southern to the northern Indian Ocean sector linked with the onset of the EASM? And what was the role of interhemispheric oceanic heat transport through the Agulhas leakage (32, 33)? Modern oceanographic observations and ocean modeling studies have recently demonstrated a tight coupling between southern hemisphere atmospheric circulation and the outflow of Indo-Pacific warm and salty waters to the Atlantic Ocean through the Agulhas leakage (32–34). This salt advection could contribute to kick-on convection and resumption of AMOC (35). The links between interhemispheric ocean and atmosphere heat transport and the final AMOC resumption remain to be fully deciphered. Modeling the sequence of events during Termination II and the last interglacial including the abrupt change in Antarctic moisture source will therefore be an excellent benchmark for Earth system models.

Material and Methods

The sequences of events during Termination I (Fig. 1) and Termination II (Fig. 2) have been established using data previously published, as described in the figure captions, complemented by our records, and improved chronologies. We have produced North Atlantic SST reconstructions (see *SI SST Reconstructions*), and measurements of EDC ice core stable isotopes (as described in the caption of Fig. 3) in order to confirm the deuterium excess shift identified in the low-resolution data (15). We have placed all the Antarctic ice core records of Termination I on a common chronology (36) coherent with the Greenland Ice Core Chronology 05 reference age scale, and all the ice core records of Termination II (including the Greenland records) on the EDC3 age scale (see *SI Text*) using gas synchronization. Termination II/last interglacial North Atlantic marine records have been placed on the EDC3 age

scale by assuming synchronous temperature changes in the air above Greenland and in the North Atlantic, hence synchronizing its SST record to the North Greenland Ice Core Project (NorthGRIP) ice $\delta^{18}O$ record and the EPICA Dome C methane record (*SI Common age scales for marine and ice records*). We have used a specific objective statistical method for the detection of deuterium excess abrupt shifts [*SI Timing of abrupt excess rise (AXR) events*].

ACKNOWLEDGMENTS. We thank T. Stocker, R. Uemura, and C. Tzedakis for discussions, as well as two anonymous reviewers. This work is a contribution to EPICA, a joint European Science Foundation/European Commission scientific program, funded by the EU (EPICA-MIS) and by national contributions from Belgium, Denmark, France, Germany, Italy, The Netherlands, Norway, Sweden, Switzerland, and the United Kingdom. The main logistic support was provided by IPEV and PNRA (at Dome C) and AWI (at Dronning Maud Land). Laboratoire des Sciences du Climat et de l'Environnement (LSCE) ice core work is funded by Agence Nationale de la Recherche through PICC and NEEM projects. This work was supported by funding to the Past4Future project from the European Commission's seventh Framework Programme, Grant 243908, and is Past4Future contribution no. 4. Contributions from R.L.E. were supported by the US National Science Foundation. This is EPICA publication 267 and LSCE publication 4166.

1. Petit JR, et al. (1999) Climate and atmospheric history of the past 420,000 years from the Vostok ice core, Antarctica. *Nature* 399:429–436.
2. Kawamura K, et al. (2007) Northern Hemisphere forcing of climatic cycles in Antarctica over the past 360,000 years. *Nature* 448:912–915.
3. Jouzel J, et al. (2007) Orbital and millenial Antarctic climate variability over the past 800,000 years. *Science* 317:793–796.
4. Masson-Delmotte V, et al. (2010) EPICA Dome C record of glacial and interglacial intensities. *Quaternary Sci Rev* 29:113–128.
5. Gherardi J-M, et al. (2009) Glacial-interglacial circulation changes inferred from 231Pa/230Th sedimentary record in the North Atlantic region. *Paleoceanography* 24:PA2204 doi: 10.1029/2008PA001696.
6. Carlson AE, et al. (2007) Geochemical proxies of North American freshwater routing during the Younger Dryas cold event. *Proc Natl Acad Sci USA* 104:6556–6561.
7. Wang Y, et al. (2008) Millennial and orbital-scale changes in the East Asian monsoon over the past 224,000 years. *Nature* 451:1090–1093.
8. Loulergue L, et al. (2008) Orbital and millenial-scale features of atmospheric CH4 over the last 800,000 years. *Nature* 453:383–386.
9. Oppo DW, McManus JF, Cullen JL (2006) Evolution and demise of the Last Interglacial warmth in the subpolar North Atlantic. *Quaternary Sci Rev* 25:3268–3277.
10. Hodell DA, et al. (2009) Surface and deep-water hydrography on Gardar Drift (Iceland Basin) during the last interglacial period. *Earth Planet Sci Lett* 288:10–19.
11. Siddall M, Bard E, Rohling EJ, Hemleben C (2006) Sea-level reversal during termination II. *Geology* 34:817–820.
12. Gouzy A, Malaize B, Pujol C, Charlier K (2004) Climatic "pause" during Termination II identified in shallow and intermediate waters off the Iberian margin. *Quaternary Sci Rev* 23:1523–1528.
13. Cheng H, et al. (2009) Ice age terminations. *Science* 326:248–252.
14. EPICA community members (2006) One-to-one coupling of glacial climate variability in Greenland and Antarctica. *Nature* 444:195–198.
15. Stenni B, et al. (2010) The deuterium excess records of EPICA Dome C and Dronning Maud Land ice cores (East Antarctica). *Quaternary Sci Rev* 29:146–159.
16. Vimeux F, Masson V, Jouzel J, Stievenard M, Petit JR (1999) Glacial-interglacial changes in ocean surface conditions in the Southern Hemisphere. *Nature* 398:410–413.
17. Stenni B, et al. (2001) An oceanic cold reversal during the last deglaciation. *Science* 293:2074–2077.
18. Uemura R, Yoshida N, Kurita N, Nakawo M, Watanabe O (2004) An observation-based method for reconstructing ocean surface changes using a 340,000 year deuterium excess record from the Dome Fuji ice core, Antarctica. *Geophys Res Lett* 31–L13216.
19. Masson-Delmotte V, et al. (2008) A review of Antarctic surface snow isotopic composition: Observations, atmospheric circulation and isotopic modelling. *J Climate* 21:3359–3387.
20. Schmidt GA, Legrande A, Hoffmann G (2007) Water isotope expressions of intrinsic and forced variability in a coupled ocean-atmosphere model. *J Geophys Res* 112:D10103 doi: 10.1029/2006JD007781.
21. Cortese G, Abelmann A, Gersonde R (2007) The last five glacial-interglacial transitions: A high resolution 450,000-year record from the subantarctic Atlantic. *Paleoceanography* 22:PA4203.
22. Barrows TT, Juggins S, De Deckker P, Calvo E, Pelejero C (2007) Long-term sea surface temperature and climate change in the Australian-New Zealand region. *Paleoceanography* 22:PA2215.
23. Govin A, et al. (2009) Evidence for northward expansion of Antarctic Bottom water mass in the Southern Ocean during the last glacial inception. *Paleoceanography* 24:PA1202 doi: 10.1029/2008PA001603.
24. Lamy F, et al. (2007) Modulation of the bipolar seesaw in the southeast Pacific during Termination I. *Earth Planet Sci Lett* 259:400–413.
25. Anderson RF, et al. (2009) Wind-driven upwelling in the Southern Ocean and the deglacial rise in atmospheric CO2. *Science* 323:1443–1448.
26. Röthlisberger R, et al. (2008) The southern hemisphere at glacial terminations: insights from the Dome C ice core. *Clim Past* 4:345–356.
27. Marshall GJ (2007) Half-century seasonal relationship between the Southern Annular Mode and Antarctic temperatures. *Int J Climatol* 27:373–383.
28. Lourantou A, Chappellaz J, Barnola JM, Masson-Delmotte V, Raynaud D Changes in atmospheric CO2 and its carbon isotopic composition during the penultimate deglaciation. *Quaternary Sci Rev*, in press.
29. Nan SL, Li JP, Yuan XJ, Zhao P (2009) Boreal spring Southern Hemisphere Annular Mode, Indian Ocean sea surface temperature, and East Asian summer monsoon. *J Geophys Res* 114:D02103 doi: 10.1029/2008JD010045.
30. Zhang R, Delworth TL (2005) Simulated tropical response to a substantial weakening of the Atlantic thermohaline circulation. *J Climate* 18:1853–1860.
31. Govin A (2008) Instability of the ocean circulation: Response of northern and southern high-latitude climate to orbital variations during the Last Interglacial and last glacial inception. PhD thesis (University of Versailles Saint Quentin (France), University of Bergen (Norway)).
32. Peeters FJC, et al. (2004) Vigourous exchange between the Indian and Atlantic oceans at the end of the past five glacial periods. *Nature* 430:661–665.
33. Sijp WP, England MH (2009) Southern Hemisphere westerly wind control over the ocean's thermohaline circulation. *J Climate* 22:1277–1286.
34. Biastoch A, Böning CW, Schwarzkopf FU, Lutjeharms JRE (2009) Increase in Agulhas leakage due to polarward shift of Southern Hemisphere westerlies. *Nature* 462:495–499.
35. Knorr G, Lohmann G (2003) Southern Ocean origin for the resumption of Atlantic thermohaline circulation during deglaciation. *Nature* 424:532–536.
36. Lemieux-Dudon B, et al. (2010) Consistent dating for Antarctica and Greenland ice cores. *Quaternary Sci Rev* 29:8–20.
37. Monnin E, et al. (2001) Atmospheric CO2 concentrations over the last glacial termination from the Dome Concordia, Antarctica, ice core. *Science* 291:112–114.
38. Waelbroeck C, et al. (2001) The timing of the last deglaciation in North Atlantic climate records, Nature. *Nature* 412:724–727.
39. Elliot M, Labeyrie L, Duplessy JC (2002) Changes in North-Atlantic deep-water formation associated with Dansgaard-Oeschger temperature oscillations (60–10 ka). *Quaternary Sci Rev* 21:1153–1165.
40. Parrenin F, et al. (2007) The EDC3 chronology for the EPICA Dome C ice core. *Clim Past* 3:485–497.